[10] J. W. Dreyer and D. Perner, J. Chem. Phys. **58**, 1195 [1973].
[11] E.-P. Röth, J. W. Dreyer, and D. Perner, unpublished results.
[12] W. Hanle and E. U. Franck, in Landolt-Börnstein, Volume 1, part 1, p. 323, Berlin 1950.
[13] R. H. Garstang, Proc. Cambridge Phil. Soc. **57**, 115 [1961].
[14] C. E. Johnson, Phys. Rev. A, **5**, 2688 [1972].
[15] A. B. Callear, Photochemistry and Reaction Kinetics, P. G. Ashmore Cambridge U.P., London 1967, Chapter 5.

Microwave Spectrum and Quadrupole Coupling Constants of 2-Chlorothiophene

J. Mjöberg and S. Ljunggren

Department of Physical Chemistry, Royal Institute of Technology, Stockholm, Sweden

(Z. Naturforsch. **28 a**, 729–738 [1973]; received 18 January 1973)

The microwave spectra of the two chlorine isotopic species of 2-chlorothiophene have been measured in the region 26 500–40 000 MHz.

For both isotopic species, the rotational constants of the ground state and one vibrationally excited state were determined, as well as the centrifugal distortion coefficients of the ground state.

From the hyperfine splitting of the rotational lines, the nuclear quadrupole coupling constants were calculated. The values in MHz are for ^{35}Cl:

$$\chi_{aa} = -74.77 \pm 0.05, \quad \chi_{bb} = 37.51 \pm 0.17, \quad \chi_{cc} = 37.25 \pm 0.18,$$

and for ^{37}Cl:

$$\chi_{aa} = -58.98 \pm 0.09, \quad \chi_{bb} = 29.55 \pm 0.26, \quad \chi_{cc} = 29.43 \pm 0.28,$$

in the principal-axes system of the molecule.

Introduction

The subject of substitution-induced ring-structure deformations has attracted the interest of many workers. In an attempt to estimate the magnitude of the effect for thiophene, Harshbarger and Bauer [1] studied 2-chlorothiophene and 2-bromothiophene by electron diffraction in the gas phase. They found that two slightly different structures, A and B, could be equally well reconciled with the experimental data. Both of these structures were distorted and did not show C_{2v} symmetry.

In a critical analysis of Harshbarger's and Bauer's work, Derissen, Kocken and van Welden [2] questioned the validity of these results. On the basis of a recalculation of Harshbarger's and Bauer's data, they claimed to have shown that a structure having C_{2v} symmetry or even a completely undistorted structure would fit the data equally well. The question regarding the amount of ring distortion in thiophene thus remained unsettled.

Table 1 shows the parameters of the different structures proposed by the above-mentioned authors together with the corresponding calculated rotational constants. From these calculations we conclude that none of the structures suggested so far will give correct values for the rotational constants unless very special values are assumed for the experimentally undetermined angles S–C–H and C–C–H. We find no reason to expect a strong deviation of these angles from those of unsubstituted thiophene. Of course, one should not anticipate that the electron diffraction and microwave results agree precisely, because of the well-known differences in the types of averages which are determined. However, the deviations between the calculated and the observed constants are probably too large to be accounted for in this way. Thus, the most reasonable conclusion seems to be that the true ring structure of 2-chlorothiophene is intermediate between the structures proposed by Harshbarger and Bauer and that of thiophene itself.

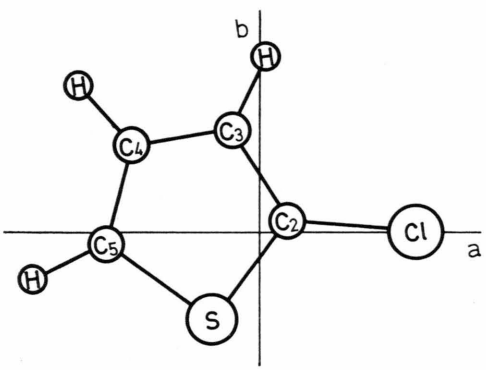

Fig. 1. 2-chlorothiophene.

Table 1. Comparison of different structures of 2-chlorothiophene.

	A Model A of HB [a]	B Model B of HB [a]	C Model B of HB [b]	D C_{2v} ring [c]	E C_{2v} ring 1 restraint [c]	F Model A refined [d]	G From thiophene [e]	H From thiophene [f]
C_2-S (Å)	1.727	1.709	1.709	1.713	1.718	1.706	1.718	1.7140
C_5-S	1.715	1.742	1.742	1.713	1.718	1.708	1.718	1.7140
C_2-C_3	1.391	1.409	1.409	1.381	1.359	1.378	1.352	1.3696
C_3-C_4	1.398	1.361	1.361	1.369	1.42	1.402	1.455	1.4232
C_4-C_5	1.359	1.380	1.380	1.381	1.359	1.355	1.352	1.3696
C−H	1.073	1.077	1.077	1.090	1.088	1.083	1.085, 1.073	1.0776, 1.0805
C_2-Cl	1.713	1.706	1.706	1.709	1.701	1.722	1.713	1.713
C_2-S-C_5 (°)	90.8	91.2	91.2	91.0	91.2	90.6	91.3	92.17
$S-C_5-C_4$	111.3	111.1	111.1	111.6	111.3	111.5	112.6	111.47
$S-C_2-C_3$	112.6	110.9	110.9	111.6	111.3	113.8	112.6	111.47
$S-C_2-Cl$	120.1	121.7	121.7	120.7	120.6	120.0	119.1	119.85
C_2-C_3-H	124.5	122.8	112.7	107	115	124.5	124.8	123.28
$S-C_5-H$	119.9	120.0	107.9	101	95	119.9	119.1	119.85
C_5-C_4-H	121.8	122.8	112.7	107	115	121.8	124.8	123.28
A (MHz)	5362.56	5353.62	5393.89	5462.67	5486.33	5405.72	5468.34	5478.85
B	1886.03	1876.09	1876.12	1892.26	1898.86	1897.30	1874.31	1866.85
C	1395.30	1389.25	1391.96	1405.42	1410.63	1404.39	1395.87	1392.47

[a] HB = Harshbarger and Bauer [1]. The H-angels where not determined by HB but were chosen by analogy with thiophene as determined by Bak et alias [4].
[b] The H-angles were chosen in order to get good agreement with the observed rotational constants.
[c] Determined by Derissen et alias [2].
[d] Determined by Derissen et alias [2]. However, they did not specify the H-angles. These were chosen to be the same as in column A.
[e] The thiophene structure was given by Bak et alias [3]. [f] The thiophene structure was given by Bak et alias [4].

Experimental

A sample of 2-chlorothiophene with 97% purity was purchased from FLUKA and used after a single redistillation at atmospheric pressure.

The microwave spectra were recorded on a Hewlett-Packard model 8460 A R-band microwave spectrometer with a phase-stabilized source oscillator.

We recorded more than 300 transitions for each of the chlorine isotopic species of 2-chlorothiophene at room temperature and pressures ranging from 8 to 50 mTorr. The frequency region was 26 500 to 40 000 MHz. The observed lines were from 0.3 to 1 MHz wide, depending on the pressure. The precision of the measured transitions was estimated to be 0.02 – 0.04 MHz.

Spectrum

The spectra of $C_4H_3{}^{32}S^{35}Cl$ and $C_4H_3{}^{32}S^{37}Cl$ were both easily observable at the natural abundances of the chlorine isotopes (75.4 and 24.6 per cent respectively).

The observable spectrum consists of a large number of $^qR_{01}$ transitions with $\Delta F = +1$. This is in good agreement with theory [5], which predicts an approximately hundredfold greater intensity for these transitions than for those with $\Delta F = 0$, while the $\Delta F = -1$ lines should have a negligible intensity. Thus, for the transitions in the *R*-band with *J*-values from 8 to 14, each rigid rotor line is split into four observable components by the quadrupole interaction.

The intensities of the absorption lines fall off as K_{-1} increases. At the same time, however, the Stark effect becomes faster. This is due to the appearance of accidental degeneracies, giving rise to first or mixed order Stark effects [6]. A genuine second-order Stark effect is obtained in some cases only, when K_{-1} has its lowest values.

In spite of the low value of the asymmetry parameter ($\varkappa = -0.758$), the high K_{-1} transitions are grouped fairly well within a few hundred MHz. As predicted by theory, the nuclear hyperfine splitting increases with K_{-1}. Thus, for low values of K_{-1}, the four quadrupole components merge into one single peak. As K_{-1} increases the peak splits into two and finally into four resolvable peaks. The dependence of the degree of splittinig on the value of K_{-1} gives rise to a very characteristic pattern.

Assignment was considerable facilitated by a special computer program which automatically plots

any desired part of the spectrum of a rigid asymmetric rotor having one quadrupole nucleus. The program is based on the usual first-order theory. It assumes that each individual absorption line has a Lorentzian shape with the same half-width for all lines. Figure 2 compares the plotted spectrum with the observed one.

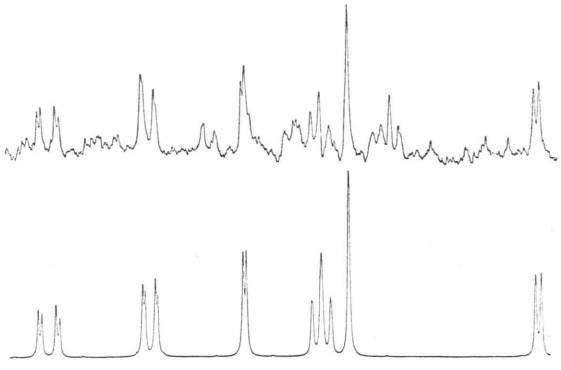

Fig. 2. Comparison of observed and computer-plotted spectrum of 2-chlorothiophene in the region 29 568 – 29 807 MHz. The differences between the two spectra are caused by Stark lobes, vibrational satellites and one ^{37}Cl line.

For the purpose of applying the plotting program, the dipole moments were calculated from an assumed structure using the CNDO/2 method [7]. This yielded $\mu_a = -2.2595$, $\mu_b = 0.2774$ and $\mu_c = 0.0$ D. The program was found particularly helpful for the ^{37}Cl isotopic species of 2-chlorothiophene, with its lower abundance and poorer signal-to-noise ratio.

A search for Q-branch transitions proved fruitless. The same thing happened with the ^{34}S species of 2-chlorothiophene. This was presumably due to the poor signal-to-noise ratio of these lines at the temperature of the experiment.

One strong vibrational satellite was observed for each of the molecules $C_4H_3{}^{32}S^{35}Cl$ and $C_4H_3{}^{32}S^{37}Cl$.

For inverting the normal matrix during the least-squares fitting process, we used the method devised by Lees [8].

The solution of the least-squares problem is usually expressed

$$\Delta x = B^{-1} A^T \Delta \nu .$$

Here B is the "normal" matrix $A^T A$ and Δx_i are the corrections to the parameters x_i. $\Delta \nu_i$ are the residuals, i. e. the differences between the observed and calculated values of the frequencies. A is the matrix of the derivatives $(A_{ij} = \partial \nu_i / \partial x_j)$.

In Lees' method, the matrix B is first scaled by the transformation

$$B_s = C B C ,$$

where

$$C = (\delta_{ij} B_{ii}{}^{-\frac{1}{2}}) .$$

This is equivalent to normalizing the fit vectors X_i [defined by $(X_i)_j = A_{ji}$] to unit length.

B_s is then diagonalized

$$\Lambda_s = O_s B_s O_s{}^T ,$$

where $\Lambda_s = (\lambda_i \delta_{ij})$ is a diagonal matrix. From elementary matrix calculations, it follows that

$$B^{-1} = C B_s{}^{-1} C = C O_s{}^T \Lambda_s{}^{-1} O_s C .$$

Obviously, we have

$$\Lambda_s{}^{-1} = (\lambda_i{}^{-1} \delta_{ij}) .$$

The diagonalization was carried out by the usual Jacobi routine.

Lees' method has two merits. It improves the conditioning of a near-singular matrix. In addition, diagonalizing the scaled matrix provides a diagnosis of linear dependences between the parameters x_i. Such dependences may be accidental, due to a limited experimental material, or they have a more fundamental origin.

Kirchhoff [9] has published a comprehensive article on centrifugal distortion effects. He discusses whether the planarity conditions should be invoked for the centrifugal distortion coefficients during the least-squares fitting process. He concludes that the planarity constraints should not be used unless the experimental data are so poor that it is not possible to fit them with five parameters.

In this investigation, a somewhat better fit was indeed obtained when the planarity constraints were released. No difficulties in the form of serious linear dependences were encountered during the fitting processes.

Table 2 lists the ground-state rotational transitions of $C_4H_3{}^{32}S^{35}Cl$ and $C_4H_3{}^{32}S^{37}Cl$. The resulting rotational, centrifugal distortion and quadrupole coupling constants are shown in Table 3. Table 4 presents the rotational constants of the first vibrational satellites and the calculated values of the vibration-rotation interaction constants.

The comparatively large relative errors in the centrifugal distortion coefficients should be viewed in relation to two factors.

1. The magnitude of the distortion effect which amounts to 0.1 – 1 MHz for most of the lines.

Table 2. Rotational transitions of 2-chlorothiophene.

Transition	$F' \leftarrow F$	$C_4H_3S^{35}Cl$ ν_{obs}	$\nu_{obs}-\nu_{calc}$	$C_4H_3S^{37}Cl$ ν_{obs}	$\nu_{obs}-\nu_{calc}$
$8_{26} \leftarrow 7_{25}$	19/2 ← 17/2			27079.03	—0.03
	17/2 ← 15/2			27078.37	—0.03
	15/2 ← 13/2			27078.19	—0.03
	13/2 ← 11/2			27078.85	—0.03
$8_{17} \leftarrow 7_{16}$	19/2 ← 17/2	26816.46	0.01		
	17/2 ← 15/2	26816.44	0.02		
	15/2 ← 13/2	26816.02	0.02		
	13/2 ← 11/2	26816.04	0.01		
$8_{35} \leftarrow 7_{34}$	19/2 ← 17/2	27007.48	—0.01		
	17/2 ← 15/2	27005.37	0.02		
	15/2 ← 13/2	27005.50	0.02		
	13/2 ← 11/2	27007.61	—0.01		
$9_{09} \leftarrow 8_{08}$	21/2 ← 19/2	26515.43	0.03		
	19/2 ← 17/2	26515.41	0.03		
	17/2 ← 15/2	26515.07	0.03		
	15/2 ← 13/2	26515.09	0.03		
$9_{27} \leftarrow 8_{26}$	21/2 ← 19/2	31377.51	0.04	30491.13	0.00
	19/2 ← 17/2	31377.01	0.03	30490.72	0.00
	17/2 ← 15/2	31376.78	0.04	30490.54	0.00
	15/2 ← 13/2	31377.28	0.04	30490.94	—0.01
$9_{45} \leftarrow 8_{44}$	21/2 ← 19/2	29907.14	—0.03	29054.50	—0.02
	19/2 ← 17/2	29904.57	—0.05	29052.46	—0.06
	17/2 ← 15/2	29904.85	—0.05	29052.68	—0.06
	15/2 ← 13/2	29907.42	—0.04	29054.72	—0.03
$9_{63} \leftarrow 8_{62}$	21/2 ← 19/2	29631.76	0.00		
	19/2 ← 17/2	29626.10	—0.03		
	17/2 ← 15/2	29627.18	—0.02		
	15/2 ← 13/2	29632.82	—0.02		
$9_{81} \leftarrow 8_{80}$	21/2 ← 19/2	29560.60	0.03		
	19/2 ← 17/2	29550.58	0.00		
	17/2 ← 15/2	29552.74	—0.03		
	15/2 ← 13/2	29562.78	0.01		
$9_{37} \leftarrow 8_{36}$	21/2 ← 19/2	29671.61	0.01		
	19/2 ← 17/2	29670.25	0.02		
	17/2 ← 15/2	29670.24	0.01		
	15/2 ← 13/2	29671.60	0.01		
$9_{73} \leftarrow 8_{72}$	21/2 ← 19/2	29588.12	—0.01		
	19/2 ← 17/2	29580.46	—0.01		
	17/2 ← 15/2	29582.02	—0.05		
	15/2 ← 13/2	29589.70	—0.02		
$9_{18} \leftarrow 8_{17}$	21/2 ← 19/2	29717.45	0.01	29031.07	0.01
	19/2 ← 17/2	29717.50	0.01	29031.09	0.01
	17/2 ← 15/2	29717.16	0.01	29030.82	0.01
	15/2 ← 13/2	29717.11	0.01	29030.80	0.01
$9_{36} \leftarrow 8_{35}$	21/2 ← 19/2	30682.68	0.02		
	19/2 ← 17/2	30681.15	0.02		
	17/2 ← 15/2	30681.16	0.02		
	15/2 ← 13/2	30682.69	0.02		
$9_{54} \leftarrow 8_{53}$	21/2 ← 19/2	29708.86	—0.01		
	19/2 ← 17/2	29704.92	—0.02		
	17/2 ← 15/2	29705.56	—0.02		
	15/2 ← 13/2	29709.50	—0.01		
$9_{72} \leftarrow 8_{71}$	21/2 ← 19/2	29588.12	—0.01		
	19/2 ← 17/2	29580.46	—0.01		
	17/2 ← 15/2	29582.02	—0.05		
	15/2 ← 13/2	29589.70	—0.02		
$9_{28} \leftarrow 8_{27}$	21/2 ← 19/2	28599.90	0.05		
	19/2 ← 17/2	28599.35	0.05		
	17/2 ← 15/2	28599.14	0.05		
	15/2 ← 13/2	28599.69	0.04		
$9_{46} \leftarrow 8_{45}$	21/2 ← 19/2	29802.88	—0.03		
	19/2 ← 17/2	29800.39	0.00		
	17/2 ← 15/2	29800.67	0.00		
	15/2 ← 13/2	29803.16	—0.03		
$9_{64} \leftarrow 8_{63}$	21/2 ← 19/2	29631.66	0.00		
	19/2 ← 17/2	29626.00	—0.03		
	17/2 ← 15/2	29627.08	—0.03		
	15/2 ← 13/2	29632.72	—0.02		

Table 2

Transition	$F' \leftarrow F$	$C_4H_3S^{35}Cl$ ν_{obs}	$\nu_{obs}-\nu_{calc}$	$C_4H_3S^{37}Cl$ ν_{obs}	$\nu_{obs}-\nu_{calc}$
$9_{82} \leftarrow 8_{81}$	21/2 ← 19/2	29560.60	0.03		
	19/2 ← 17/2	29550.58	0.00		
	17/2 ← 15/2	29552.75	—0.02		
	15/2 ← 13/2	29562.78	0.01		
$10_{9,10} \leftarrow 9_{09}$	23/2 ← 21/2	29267.89	0.01	28617.23	—0.02
	21/2 ← 19/2	29267.86	0.01	28617.21	—0.02
	19/2 ← 17/2	29267.59	0.01	28616.99	—0.02
	17/2 ← 15/2	29267.62	0.01	28617.01	—0.02
$10_{28} \leftarrow 9_{27}$	23/2 ← 21/2	34750.69	—0.01	33804.94	0.02
	21/2 ← 19/2	34750.41	—0.01	33804.70	0.02
	19/2 ← 17/2	34750.19	—0.01	33804.53	0.02
	17/2 ← 15/2	34750.47	—0.01	33804.77	0.02
$10_{46} \leftarrow 9_{45}$	23/2 ← 21/2	33387.71	0.02	32417.31	0.00
	21/2 ← 19/2	33385.83	0.04	32415.83	0.00
	19/2 ← 17/2	33385.96	0.03	32415.93	0.00
	17/2 ← 15/2	33387.84	0.02	32417.41	—0.01
$10_{64} \leftarrow 9_{63}$	23/2 ← 21/2	32966.10	0.00	32054.84	0.07
	21/2 ← 19/2	32961.99	—0.01	32051.56	0.02
	19/2 ← 17/2	32962.64	—0.01	32052.07	0.02
	17/2 ← 15/2	32966.75	0.00	32055.35	0.07
$10_{82} \leftarrow 9_{81}$	23/2 ← 21/2	32867.06	—0.03		
	21/2 ← 19/2	32859.84	0.02		
	19/2 ← 17/2	32861.18	—0.01		
	17/2 ← 15/2	32868.47	0.00		
$10_{1,10} \leftarrow 9_{19}$	23/2 ← 21/2	29183.78	0.02	28520.19	—0.01
	21/2 ← 19/2	29183.69	0.02	28520.12	—0.01
	19/2 ← 17/2	29183.43	0.02	28519.91	—0.02
	17/2 ← 15/2	29183.52	0.02	28519.98	—0.02
$10_{38} \leftarrow 9_{37}$	23/2 ← 21/2	32908.26	—0.04		
	21/2 ← 19/2	32907.33	0.00		
	19/2 ← 17/2	32907.27	0.00		
	17/2 ← 15/2	32908.20	—0.04		
$10_{56} \leftarrow 9_{55}$	23/2 ← 21/2	33063.95	0.00	32142.50	0.01
	21/2 ← 19/2	33061.15	0.06	32140.26	0.03
	19/2 ← 17/2	33061.51	0.05	32140.55	0.03
	17/2 ← 15/2	33064.31	—0.01	32142.79	0.02
$10_{74} \leftarrow 9_{73}$	23/2 ← 21/2	32905.45	—0.01		
	21/2 ← 19/2	32899.91	0.02		
	19/2 ← 17/2	32900.88	0.01		
	17/2 ← 15/2	32906.45	0.00		
$10_{92} \leftarrow 9_{91}$	23/2 ← 21/2	32841.24	0.00	31943.70	0.03
	21/2 ← 19/2	32832.04	0.00	31936.44	0.02
	19/2 ← 17/2	32833.82	—0.04	31937.88	0.03
	17/2 ← 15/2	32843.08	0.02	31945.09	—0.02
$10_{19} \leftarrow 9_{18}$	23/2 ← 21/2	32500.83	—0.02	31780.92	0.06
	21/2 ← 19/2	32500.90	—0.01	31780.97	0.06
	19/2 ← 17/2	32500.62	—0.02	31780.75	0.06
	17/2 ← 15/2	32500.55	—0.02	31780.70	0.05
$10_{37} \leftarrow 9_{36}$	23/2 ← 21/2	34419.50	0.04	33352.77	0.01
	21/2 ← 19/2	34418.36	0.02	33351.84	—0.04
	19/2 ← 17/2	34418.31	0.02	33351.80	—0.04
	17/2 ← 15/2	34419.45	0.04	33352.73	0.01
$10_{55} \leftarrow 9_{54}$	23/2 ← 21/2	33076.17	—0.04	32151.53	0.03
	21/2 ← 19/2	33073.36	0.02	32149.22	—0.02
	19/2 ← 17/2	33073.72	0.01	32149.51	—0.02
	17/2 ← 15/2	33076.53	—0.04	32151.82	0.04
$10_{73} \leftarrow 9_{72}$	23/2 ← 21/2	32905.46	—0.01		
	21/2 ← 19/2	32899.92	0.03		
	19/2 ← 17/2	32900.89	0.01		
	17/2 ← 15/2	32906.46	0.01		
$10_{91} \leftarrow 9_{90}$	23/2 ← 21/2	32841.24	0.00	31943.70	0.03
	21/2 ← 19/2	32832.04	0.00	31936.44	0.02
	19/2 ← 17/2	32833.82	—0.04	31937.88	0.03
	17/2 ← 15/2	32843.08	0.02	31945.09	—0.02
$10_{29} \leftarrow 9_{28}$	23/2 ← 21/2	31572.25	0.00		
	21/2 ← 19/2	31571.87	0.00		
	19/2 ← 17/2	31571.65	0.00		
	17/2 ← 15/2	31527.06	0.00		

Table 2

Transition	$F' \leftarrow F$	$C_4H_3S^{35}Cl$ ν_{obs}	$\nu_{obs}-\nu_{calc}$	$C_4H_3S^{37}Cl$ ν_{obs}	$\nu_{obs}-\nu_{calc}$
$10_{47} \leftarrow 9_{46}$	23/2 ← 21/2	33170.70	—0.04	32245.56	0.01
	21/2 ← 19/2	33168.86	—0.05	32244.14	0.03
	19/2 ← 17/2	33168.99	—0.04	32244.24	0.03
	17/2 ← 15/2	33170.83	—0.03	32245.66	0.01
$10_{65} \leftarrow 9_{64}$	23/2 ← 21/2	32965.72	—0.02	32054.59	0.07
	21/2 ← 19/2	32961.59	—0.05	32051.32	0.03
	19/2 ← 17/2	32962.24	—0.05	32051.83	0.03
	17/2 ← 15/2	32966.37	—0.02	32055.10	0.07
$10_{83} \leftarrow 9_{82}$	23/2 ← 21/2	32867.06	—0.03		
	21/2 ← 19/2	32859.84	0.02		
	19/2 ← 17/2	32861.18	—0.01		
	17/2 ← 15/2	32868.47	0.00		
$11_{29} \leftarrow 10_{28}$	25/2 ← 23/2	37988.45	—0.01	37000.40	0.01
	23/2 ← 21/2	37988.32	0.00	37000.28	0.02
	21/2 ← 19/2	37988.12	0.00	37000.12	0.01
	19/2 ← 17/2	37988.25	—0.01	37000.25	0.02
$11_{47} \leftarrow 10_{46}$	25/2 ← 23/2	36945.97	—0.03	35846.20	—0.03
	23/2 ← 21/2	36944.50	—0.04	35845.12	0.03
	21/2 ← 19/2	36944.55	—0.04	35845.16	0.03
	19/2 ← 17/2	36946.02	—0.03	35846.24	—0.03
$11_{65} \leftarrow 10_{64}$	25/2 ← 23/2			35306.32	0.01
	23/2 ← 21/2			35303.93	0.05
	21/2 ← 19/2			35304.25	0.06
	19/2 ← 17/2			35306.63	0.01
$11_{83} \leftarrow 10_{82}$	25/2 ← 23/2	36181.37	—0.01	35188.01	0.01
	23/2 ← 21/2	36175.94	0.02	35183.64	—0.06
	21/2 ← 19/2	36176.83	0.01	35184.35	—0.05
	19/2 ← 17/2	36182.28	0.01	35188.72	0.01
$11_{10,1} \leftarrow 10_{10,0}$	25/2 ← 23/2			35135.06	0.04
	23/2 ← 21/2			35128.31	0.01
	21/2 ← 19/2			35129.50	—0.01
	19/2 ← 17/2			35136.24	0.01
$11_{1,11} \leftarrow 10_{1,10}$	25/2 ← 23/2	31981.17	—0.02		
	23/2 ← 21/2	31981.10	—0.02		
	21/2 ← 19/2	31980.88	—0.02		
	19/2 ← 17/2	31980.95	—0.02		
$11_{39} \leftarrow 10_{38}$	25/2 ← 23/2	36099.46	0.01		
	23/2 ← 21/2	36098.76	0.01		
	21/2 ← 19/2	36098.67	0.01		
	19/2 ← 17/2	36099.37	0.01		
$11_{57} \leftarrow 10_{56}$	25/2 ← 23/2	36439.97	0.05		
	23/2 ← 21/2	36437.80	0.03		
	21/2 ← 19/2	36438.01	0.04		
	19/2 ← 17/2	36440.18	0.06		
$11_{75} \leftarrow 10_{74}$	25/2 ← 23/2	36232.89	—0.01		
	23/2 ← 21/2	36228.73	0.02		
	21/2 ← 19/2	36229.35	0.01		
	19/2 ← 17/2	36233.54	0.02		
$11_{93} \leftarrow 10_{92}$	25/2 ← 23/2	36146.54	—0.02		
	23/2 ← 21/2	36139.64	—0.02		
	21/2 ← 19/2	36140.85	0.00		
	19/2 ← 17/2	36147.76	0.01		
$11_{1,10} \leftarrow 10_{19}$	25/2 ← 23/2	35211.63	—0.02	34449.79	—0.06
	23/2 ← 21/2	35211.68	—0.02	34449.83	—0.06
	21/2 ← 19/2	35211.45	—0.02	34449.65	—0.06
	19/2 ← 17/2	35211.40	—0.02	34449.61	—0.06
$11_{38} \leftarrow 10_{37}$	25/2 ← 23/2	38163.53	0.00		
	23/2 ← 21/2	38162.68	—0.04		
	21/2 ← 19/2	38162.60	—0.03		
	19/2 ← 17/2	38163.45	0.01		
$11_{56} \leftarrow 10_{55}$	25/2 ← 23/2	36469.88	—0.02	35441.54	0.00
	23/2 ← 21/2	36467.71	—0.03	35439.83	—0.01
	21/2 ← 19/2	36467.92	—0.03	35439.99	—0.01
	19/2 ← 17/2	36470.09	—0.02	35441.70	0.00
$11_{74} \leftarrow 10_{73}$	25/2 ← 23/2	36232.91	—0.01		
	23/2 ← 21/2	36228.75	0.01		
	21/2 ← 19/2	36229.37	0.00		
	19/2 ← 17/2	36233.56	0.01		

Table 2

Transition	$F' \leftarrow F$	$C_4H_3S^{35}Cl$ ν_{obs}	$\nu_{obs}-\nu_{calc}$	$C_4H_3S^{37}Cl$ ν_{obs}	$\nu_{obs}-\nu_{calc}$
$11_{92} \leftarrow 10_{91}$	25/2 ← 23/2	36146.54	—0.02		
	23/2 ← 21/2	36139.64	—0.02		
	21/2 ← 19/2	36140.85	0.00		
	19/2 ← 17/2	36147.76	0.01		
$11_{2,10} \leftarrow 10_{29}$	25/2 ← 23/2	34499.80	0.03	33678.54	—0.03
	23/2 ← 21/2	34499.53	0.03	33678.33	—0.02
	21/2 ← 19/2	34499.36	0.03	33678.20	—0.01
	19/2 ← 17/2	34499.63	0.03	33678.41	—0.02
$11_{48} \leftarrow 10_{47}$	25/2 ← 23/2	36536.55	0.04	35519.37	—0.03
	23/2 ← 21/2	36535.18	0.03	35518.32	—0.01
	21/2 ← 19/2	36535.22	0.03	35518.35	—0.01
	19/2 ← 17/2	36536.59	0.03	35519.40	—.004
$11_{66} \leftarrow 10_{65}$	25/2 ← 23/2			35305.51	—0.01
	23/2 ← 21/2			35303.10	0.01
	21/2 ← 19/2			35303.42	0.02
	19/2 ← 17/2			35305.83	0.00
$11_{84} \leftarrow 10_{83}$	25/2 ← 23/2	36181.37	—0.01	35188.01	0.01
	23/2 ← 21/2	36175.94	0.02	35183.64	—0.06
	21/2 ← 19/2	36176.83	0.01	35184.35	—0.05
	19/2 ← 17/2	36182.28	0.01	35188.72	0.01
$11_{10,2} \leftarrow 10_{10,1}$	25/2 ← 23/2			35135.06	0.04
	23/2 ← 21/2			35128.31	0.01
	21/2 ← 19/2			35129.50	—0.01
	19/2 ← 17/2			35136.24	0.01
$12_{0,12} \leftarrow 11_{0,11}$	27/2 ← 25/2			34021.25	—0.03
	25/2 ← 23/2			34021.22	—0.03
	23/2 ← 21/2			34021.07	—0.03
	21/2 ← 19/2			34021.10	—0.03
$12_{48} \leftarrow 11_{47}$	27/2 ← 25/2			39356.62	—0.01
	25/2 ← 23/2			39355.72	0.00
	23/2 ← 21/2			39355.73	0.00
	21/2 ← 19/2			39356.63	0.00
$12_{66} \leftarrow 11_{65}$	27/2 ← 25/2			38571.95	—0.06
	25/2 ← 23/2			38570.14	0.00
	23/2 ← 21/2			38570.33	—0.01
	21/2 ← 19/2			38572.15	—0.06
$12_{84} \leftarrow 11_{83}$	27/2 ← 25/2	39504.10	—0.01	38416.71	—0.02
	25/2 ← 23/2	39499.91	0.00	38413.43	0.01
	23/2 ← 21/2	39500.52	0.02	38413.89	0.00
	21/2 ← 19/2	39504.70	0.00	38417.17	—0.03
$12_{10,2} \leftarrow 11_{10,1}$	27/2 ← 25/2	39426.30	—0.01	38347.46	—0.03
	25/2 ← 23/2	39419.76	0.00	38342.34	0.02
	23/2 ← 21/2	39420.81	0.00	38343.15	0.01
	21/2 ← 19/2	39427.35	—0.01	38348.31	0.00
$12_{1,12} \leftarrow 11_{1,11}$	27/2 ← 25/2			33986.77	—0.07
	25/2 ← 23/2			33986.73	—0.06
	23/2 ← 21/2			33986.58	—0.07
	21/2 ← 19/2			33986.62	—0.07
$12_{3,10} \leftarrow 11_{39}$	27/2 ← 25/2	39238.69	—0.03	38230.57	0.00
	25/2 ← 23/2	39238.17	—0.03	38230.15	0.00
	23/2 ← 21/2	39238.08	—0.02	38230.08	0.00
	21/2 ← 19/2	39238.60	—0.02	38230.50	0.01
$12_{58} \leftarrow 11_{57}$	27/2 ← 25/2	39831.08	0.01	38710.84	0.00
	25/2 ← 23/2	39829.42	0.01	38709.51	—0.02
	23/2 ← 21/2	39829.53	0.00	38709.60	—0.02
	21/2 ← 19/2	39831.19	0.00	38710.93	0.00
$12_{76} \leftarrow 11_{75}$	27/2 ← 25/2	39571.39	—0.02	38476.52	—0.01
	25/2 ← 23/2	39568.20	0.01	38474.01	0.02
	23/2 ← 21/2	39568.61	0.01	38474.33	0.01
	21/2 ← 19/2	39571.80	—0.02	38476.84	—0.02
$12_{94} \leftarrow 11_{93}$	27/2 ← 25/2	39458.59	0.01	38376.20	—0.03
	25/2 ← 23/2	39453.28	0.01	38372.02	—0.02
	23/2 ← 21/2	39454.09	0.01	38372.68	0.00
	21/2 ← 19/2	39459.39	0.00	38376.86	—0.01
$12_{11,2} \leftarrow 11_{11,1}$	27/2 ← 25/2			38326.33	—0.01
	25/2 ← 23/2			38320.07	—0.02
	23/2 ← 21/2			38321.11	—0.01
	21/2 ← 19/2			38327.40	0.03

Table 2

Transition	$F' \leftarrow F$	$C_4H_3S^{35}Cl$ ν_{obs}	$\nu_{obs}-\nu_{calc}$	$C_4H_3S^{37}Cl$ ν_{obs}	$\nu_{obs}-\nu_{calc}$
$12_{1,11} \leftarrow 11_{1,10}$	27/2 ← 25/2	37896.79	0.00	37081.51	−0.04
	25/2 ← 23/2	37896.81	0.00	37081.53	−0.04
	23/2 ← 21/2	37896.63	0.00	37081.38	−0.04
	21/2 ← 19/2	37896.61	0.00	37081.36	−0.04
$12_{57} \leftarrow 11_{56}$	27/2 ← 25/2	39897.61	−0.03	38760.11	0.01
	25/2 ← 23/2	39895.93	−0.03	38758.79	0.01
	23/2 ← 21/2	39896.04	−0.04	38758.88	0.01
	21/2 ← 19/2	39897.72	−0.04	38760.20	0.01
$12_{75} \leftarrow 11_{74}$	27/2 ← 25/2	39571.48	−0.02	38476.58	−0.01
	25/2 ← 23/2	39568.29	0.01	38474.07	0.02
	23/2 ← 21/2	39568.70	0.01	38474.39	0.01
	21/2 ← 19/2	39571.89	−0.02	38476.90	−0.02
$12_{93} \leftarrow 11_{92}$	27/2 ← 25/2	39458.59	0.01	38376.20	−0.03
	25/2 ← 23/2	39453.28	0.01	38372.02	−0.02
	23/2 ← 21/2	39454.09	0.01	38372.68	0.00
	21/2 ← 19/2	39459.39	0.00	38376.86	−0.01
$12_{11,1} \leftarrow 11_{11,0}$	27/2 ← 25/2			38326.33	−0.01
	25/2 ← 23/2			38320.07	−0.02
	23/2 ← 21/2			38321.11	−0.01
	21/2 ← 19/2			38327.40	0.03
$12_{49} \leftarrow 11_{48}$	27/2 ← 25/2	39889.76	0.00	38785.21	0.00
	25/2 ← 23/2	39888.72	0.00	38784.36	−0.02
	23/2 ← 21/2	39888.72	0.00	38784.36	−0.02
	21/2 ← 19/2	39889.76	0.01	38785.21	0.01
$12_{67} \leftarrow 11_{66}$	27/2 ← 25/2	39676.31	0.05	38569.79	−0.01
	25/2 ← 23/2	39673.90	0.02	38567.96	0.03
	23/2 ← 21/2	39674.15	0.02	38568.16	0.04
	21/2 ← 19/2	39676.55	0.05	38569.99	−0.01
$12_{85} \leftarrow 11_{84}$	27/2 ← 25/2	39504.10	−0.01	38416.71	−0.02
	25/2 ← 23/2	39499.91	0.01	38413.43	0.01
	23/2 ← 21/2	39500.52	0.02	38413.89	0.00
	21/2 ← 19/2	39504.70	0.00	38417.17	−0.03
$12_{10,3} \leftarrow 11_{10,2}$	27/2 ← 25/2	39426.30	−0.01	38347.46	−0.03
	25/2 ← 23/2	39419.76	0.00	38342.34	0.02
	23/2 ← 21/2	39420.81	0.00	38343.15	0.01
	21/2 ← 19/2	39427.35	−0.01	38348.31	0.00
$13_{0,13} \leftarrow 12_{0,12}$	29/2 ← 27/2	37575.43	0.04	36732.36	0.04
	27/2 ← 25/2	37575.39	0.04	36732.33	0.04
	25/2 ← 23/2	37575.23	0.04	36732.20	0.03
	23/2 ← 21/2	37575.27	0.04	36732.22	0.03
$13_{1,13} \leftarrow 12_{1,12}$	29/2 ← 27/2	37559.43	0.02		
	27/2 ← 25/2	37559.38	0.02		
	25/2 ← 23/2	37559.22	0.02		
	23/2 ← 21/2	37559.27	0.02		
$13_{2,12} \leftarrow 12_{2,11}$	29/2 ← 27/2			39312.42	0.05
	27/2 ← 25/2			39312.30	0.05
	25/2 ← 23/2			39312.19	0.05
	23/2 ← 21/2			39312.31	0.05

2. Only $^qR_{01}$-transitions in a limited frequency region were included in the fit. Møllendal and Marstokk [10] emphasized the importance of including as many different types of transitions as possible in the fit, if accurate values of the distortion coefficients are to be obtained.

The evaluation of the frequencies of the low K_{-1} transitions had to be performed at the highest Stark voltage available (approx. 4000 V/cm) owing to the low Stark effect of these lines. Low Stark voltages result in incomplete modulation of these lines producing an apparent frequency displacement.

Table 3. Rotational constants (MHz), principal moments of inertia (amu Å^2) and centrifugal distortion coefficients (Hz) of the two isotopic species of 2-chlorothiophene.

	$C_4H_3S^{35}Cl$	$C_4H_3S^{37}Cl$
A	5396.039 ± 0.025	5395.819 ± 0.037
B	1875.224 ± 0.002	1818.821 ± 0.002
C	1391.162 ± 0.002	1359.835 ± 0.002
$\varkappa$	−0.758	−0.773
I_a	93.65703 ± 0.00044	93.66085 ± 0.00064
I_b	269.50228 ± 0.00020	277.85964 ± 0.00029
I_c	363.27691 ± 0.00034	371.64591 ± 0.00049
$\Delta = I_c - I_a - I_b$	0.11760 ± 0.00059	0.12542 ± 0.00086
Δ_J	79.5 ± 3.0	80.1 ± 4.9
Δ_{JK}	843 ± 14	794 ± 19
Δ_K	5324 ± 2894	−7924 ± 3918
δ_J	10.5 ± 2.2	40.0 ± 3.1
δ_K	496 ± 127	167 ± 157

Table 4. Rotational constants (MHz), principal moments of inertia (amu Å^2) of the first vibrational satellites and vibration-rotation interaction constants of 2-chlorothiophene.

	$C_4H_3S^{35}Cl$	$C_4H_3S^{37}Cl$
A	5346.45 ± 1.53	5343.75 ± 5.34
B	1876.33 ± 0.04	1819.92 ± 0.16
C	1392.65 ± 0.03	1361.33 ± 0.17
I_a	94.526 ± 0.027	94.573 ± 0.095
I_b	269.343 ± 0.006	277.692 ± 0.024
I_c	362.888 ± 0.009	371.237 ± 0.046
$\Delta = I_c - I_a - I_b$	−0.981 ± 0.029	−1.028 ± 0.108
α_a	−49.587	−52.050
α_b	1.106	1.101
α_c	1.490	1.497

Figure 3 shows an incompletely modulated line as simulated by a computer. Our experiments verified that the observed frequencies of the transitions were indeed displaced when the Stark voltage was varied. The order of magnitude of this displacement was 0.05 − 0.2 MHz. No attempt was made to correct theoretically for this effect since only a few of the lines concerned have a genuine second-order Stark effect [6].

Owing to the high J-values and low Stark effect of the unsplit lines measured, we could not determine the dipole moment.

As we have already mentioned, one strong vibrational satellite was observed for each isotopic species. A rather crude estimate yielded the value 0.327 for the intensity ratio of the vibrational satellite to

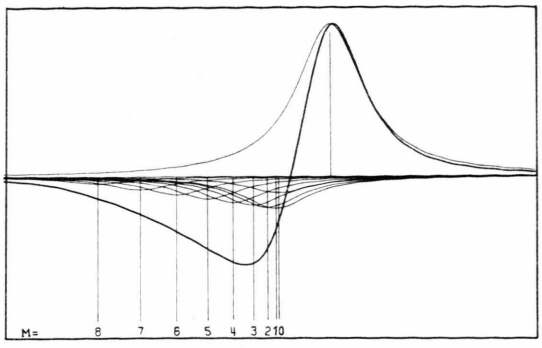

Fig. 3. Computer-plotted shape of an incompletely modulated line showing the original line, the Stark lobes for different M values and the resulting distorted line shape.

the ground state at 24.1 °C. From this, the energy difference was calculated to be 231 cm^{-1}. The large negative change of the inertia defect in going from the ground to the vibrationally excited state is typical for an out-of-plane vibration [11–13].

The spectroscopic vibration-rotation constant α_a has a large negative value in contrast to α_b and α_c. This indicates that the vibration is probably an out-of-plane C – Cl bending vibration, since the a principal axis of the molecule is directed approximately along the C – Cl bond.

Starting from the well-known expression for the inertia defect of Oka and Morino [14], Kakar [15] has shown that as the frequencies of all in-plane vibrational modes tend to infinity, the frequency of the out-of-plane vibration can be calculated from the formula

$$\omega_t = h/2\,\pi^2\,c\,(\Delta_0 - \Delta_1),$$

where Δ_0 and Δ_1 are the inertial defects of the ground and the first out-of-plane excited states. Inserting the values for Δ_0 and Δ_1, we obtain

$$\omega_t = 61.4\ cm^{-1}.$$

This deviates largely from the earlier value of 231 cm^{-1} as estimated from the intensity ratio. The deviation indicates the presence of strong interaction with low frequency in-plane vibrations.

These conclusions are in very good qualitative agreement with the results of infrared spectroscopic studies [16, 17]. According to these studies there are two absorption lines in the far infrared region, one at 222 cm^{-1} and the other at 257 cm^{-1}. The first line is interpreted as an out-of-plane vibration involving the chlorine atom and the second one as an in-plane vibration also involving the chlorine atom.

Molecular Structure

Table 1 lists the parameters and rotational constants of the different structural models suggested on the basis of electron diffraction measurements. HB(A) and HB(B) are the original structures proposed by Harshbarger and Bauer [1]. The remaining structures except G and H, which are based on the ring structure of unsubstituted thiophene, are those suggested by Derissen et alias [2]. They include two structures with C_{2v} symmetry (one of which has the additional constraint that the $C_3 - C_4$ distance should be equal to that of thiophene) and a "refined" version of HB(A). Incidentally, the two C_{2v} structures are the only ones for which the positions of the hydrogen atoms were actually calculated from the electron diffraction data. For the remaining structures we had to assume values for the C – C – H and S – C – H angles.

We first observe that the two C_{2v} structures of Derissen et al. yield poor results for the rotational constants. This is presumably due to the fact that the assumed high symmetry imposes unduly stringent conditions on the fitting process with the result that the hydrogen angles are forced to assume unreasonable values.

For most of the remaining structures we can achieve good agreement with the experimental rotational constants simply by choosing suitable values for the hydrogen angles. This is nicely illustrated for structure C where the agreement with experiment is almost perfect.

If, on the other hand, we accept that the hydrogen angles should not deviate too much from those of thiophene itself, the conclusion becomes different. The observed rotational constant A is larger than the calculated values for the structures A and B and smaller than the calculated values for the structures G and H, which are based on the structure of thiophene. If we assume this to be significant in spite of the principal difficulties in comparing electron diffraction and microwave results, we conclude that the true ring structure of 2-chlorothiophene will probably lie somewhere between the structures proposed by Harshbarger and Bauer and that of thiophene.

Quadrupole Interaction

The off-diagonal elements of the quadrupole coupling tensor cannot usually be determined from ex-

periment since these elements do not contribute to the first-order quadrupole splitting. This usually means that χ cannot be diagonalized to obtain its principal elements, χ_x, χ_y and χ_z, without some kind of additional assumption.

The usual approach [18] is to assume that the direction of the z principal axis of the quadrupole tensor coincides with the direction of the C – Cl bond. The y-direction is assumed to be perpendicular to the plane of the molecule. Let us denote by θ the angle between the z-axis and the a principal axis of the rotating molecule. The following expressions for the quadrupole coupling tensor components are then obtained for a planar molecule:

$$\chi_x = (\chi_{bb}\cos^2\theta - \chi_{aa}\sin^2\theta)/(\cos^2\theta - \sin^2\theta),$$
$$\chi_y = \chi_{cc},$$
$$\chi_z = (\chi_{aa}\cos^2\theta - \chi_{bb}\sin^2\theta)/(\cos^2\theta - \sin^2\theta).$$

The asymmetry parameter η is defined in the following way

$$\eta = (\chi_x - \chi_y)/\chi_z .$$

Another asymmetry parameter, Δ_m, was defined by Goldstein [19] as

$$\Delta_m = \chi_x - \chi_y .$$

The experimental results for the quadrupole coupling coefficients are listed in Table 5.

The ratio of the principal components of the quadrupole coupling tensor of $C_3H_4S^{37}Cl$ to those of $C_3H_4S^{35}Cl$ is 0.7878, 0.7899 and 0.7888 for χ_x, χ_y and χ_z, respectively. These values are very close to the theoretical ratio of the quadrupole moments, 0.7881. They deviate by less than 3 parts per thousand.

Let us identify the p-orbital populations U_x, U_y and U_z with the bond order matrix elements $P_{p_xp_x}$, $P_{p_yp_y}$ and $P_{p_zp_z}$. We obtain for the excess p-orbital electron densities [20]

$$f_x = U_x - \tfrac{1}{2}(U_y + U_z) = P_{p_xp_x} - \tfrac{1}{2}(P_{p_yp_y} + P_{p_zp_z}),$$

etc. The components of the quadrupole coupling tensor can be estimated from the relations

$$\chi_x = f_x (e\,Q\,q)_{\mathrm{at}},$$

where $(e\,Q\,q)_{\mathrm{at}}$ is the coupling constant of one unbalanced electron. For ^{35}Cl it is usually taken as 109.746 MHz [5].

The above relations can easily be derived from molecular orbital theory. A number of authors have given similar derivations [20–25]. The instantaneous value of the diagonal element $q_i = \partial^2 V/\partial x_i^2$ of the field gradient tensor is given by the expression

$$q_i = \sum_l (3\cos^2\theta_l^{(i)} - 1)\, r_l ,$$

where the summation includes all electrons, and where $\theta_l^{(i)}$ is the angle between the x-axis and the position vector of the electron, $\boldsymbol{r}_l$.

If the wave function Ψ of the system is assumed to have the form of a single Slater-determinant over the spin-orbitals Ψ_μ, and if the latter are expressed as linear combinations of atomic orbitals Φ_i:

$$\Psi_\mu = \sum_i c_{i\mu}\,\Phi_i ,$$

the following relations are obtained for the quantum mechanical mean value of q_i:

$$\langle q_i\rangle_\Psi = \langle \Psi \,|\, \sum_l (3\cos^2\theta_l^{(i)} - 1)\, r_l^{-3} \,|\, \Psi\rangle$$
$$= \sum_\mu \langle \Psi_\mu \,|\, (3\cos^2\theta_l^{(i)} - 1)\, r_l^{-3} \,|\, \Psi_\mu\rangle ,$$

by virtue of the fact that q_i is a sum of one-electron operators. Inserting the expansion for Ψ_μ we finally obtain

$$\langle q_i\rangle_\Psi = \sum_{j,k} P_{jk}\, q_{jk}^{(i)} ,$$

Table 5. Nuclear quadrupole coupling constants (MHz) in 2-chlorothiophene. The letters A and B refer to the structures in Table 1.

	2-chlorothiophene, ^{35}Cl		2-chlorothiophene, ^{37}Cl	
	A	B	A	B
χ_x	38.90 ± 0.18	38.68 ± 0.18	30.64 ± 0.27	30.17 ± 0.27
χ_y	37.25 ± 0.18	37.25 ± 0.18	29.43 ± 0.28	29.43 ± 0.28
χ_z	−76.15 ± 0.05	−75.54 ± 0.05	−60.07 ± 0.09	−59.59 ± 0.09
η	−0.0216	−0.0137	−0.0203	−0.0124
θ_{za}	6.30°	4.74°	6.30°	4.74°
χ_{aa}	−74.77 ± 0.05		−58.98 ± 0.09	
χ_{bb}	37.51 ± 0.17		29.55 ± 0.26	
χ_{cc}	37.25 ± 0.18		29.43 ± 0.28	

where $P_{jk} = \sum_{\mu} c_{j\mu} c_{k\mu}$ is the bond order matrix and

$$q_{jk}^{(i)} = \langle \Phi_j(l) | (3\cos^2\theta_l^{(i)} - 1)\, r_l^{-3} | \Phi_k(l) \rangle .$$

Neglecting all except the diagonal elements of $q^{(i)}$ between p-orbitals on the quadrupole atom and utilizing the fact that

$$q_{kk}^{(i)} \rangle = -\tfrac{1}{2}\, q_{ii}^{(i)}, \qquad (k \neq i)$$

we obtain

$$\langle q_i \rangle_{\Psi} = \sum_k P_{kk}\, q_{kk}^{(i)} = [P_{ii} - \tfrac{1}{2}\,(P_{kk} + P_{ll})]\, q_{\mathrm{at}} ,$$

where i, k and l now stand for the orbitals p_x, p_y and p_z. Finally.

$$\chi_{ii} = [P_{ii} - \tfrac{1}{2}\,(P_{kk} + P_{ll})]\, e\,Q\, q_{\mathrm{at}} .$$

In particular, we may express the Goldstein [19] asymmetry parameter, Δ_m, in the form

$$\Delta_m = \chi_x - \chi_y = \tfrac{3}{2}\,(P_{xx} - P_{yy})\, e\,Q\, q_{\mathrm{at}} .$$

According to Goldstein, the amount of double bond character is given by the expression

$$\delta = \Delta_m / \Delta_{\mathrm{at}} ,$$

where $\Delta_{\mathrm{at}} = (3/2)\, e\,Q\, q_{\mathrm{at}}$. Thus, in terms of the bond order matrices,

$$\delta = P_{xx} - P_{yy} .$$

We should not expect, a priori, that the derived equations will hold very accurately. To begin with, we have neglected electron-correlation and core-polarization effects. Moreover, it is generally recognized that the orbital coefficients obtained by the CNDO method do not necessarily represent the best possible choice, in view of the semi-empirical nature of the method. Betsuyaku [20] has tried to obtain an improved set of orbital coefficients by applying a Löwdin type transformation [26] to the orbital coefficients obtained by the CNDO method.

From our CNDO/2 calculations on 2-chlorothiophene, the following values were obtained:

$P_{xx} = 1.9849$, $P_{yy} = 1.9706$ and $P_{zz} = 1.0666$.

These correspond to a double-bond character of the C – Cl bond equal to 1.43 per cent, since

$$\delta = P_{xx} - P_{yy} = 0.0143 .$$

The experimental value calculated from Goldstein's formula is $\delta = 0.0063$. However, it is important to bear in mind the very weak dependence of the quadrupole splittings of the investigated transitions on the constants χ_{bb} and χ_{cc}. These constants are therefore extremely sensitive to very small systematic errors in the measurements. (Such errors may arise in evaluating the unresolved splittings, or from the interference of the lines with the Stark components of nearby transitions.) Thus, changing χ_{bb} by 1 MHz will cause only a negligible change of the splittings of the completely resolved lines and a change of the order of 0.02 MHz in the unresolved or incompletely resolved lines. This figure is of the same order as the error of measurement. It is evident that in the case of the present investigation, little reliance can be attached to Goldstein's Δ_m, obtained as the difference between χ_x and χ_y .Improved values of these constants could be obtained by extending the measurements to a lower frequency region where the quadrupole splittings are greater.

With the usual value 109.746 MHz for $e\,Q\,q_{\mathrm{at}}$ and applying the above formula for the components of the quadrupole tensor in terms of the bond order matrices, our CNDO/2 calculation yields

$\chi_x = 51.18$, $\chi_y = 48.82$ and $\chi_z = 100.00$ MHz.

However, we found much better agreement with the experimental result for the quadrupole coupling tensor by assuming that $e\,Q\,q_{\mathrm{at}} = 83.58$ MHz. This yields

$\chi_x = 38.97$, $\chi_y = 37.18$ and $\chi_z = -76.16$ MHz.

[1] W. R. Harshbarger and S. H. Bauer, Acta Cryst. B **26**, 1010 [1970].
[2] J. L. Derissen, J. W. M. Kocken, and R. H. van Welden, Acta Cryst. B **27**, 1692 [1971].
[3] B. Bak, D. Christensen, J. Rastrup-Andersen, and U. E. Tannenbaum, J. Chem. Phys. **25**, 892 [1956].
[4] B. Bak, D. Christensen, L. Hansen-Nygaard, and J. Rastrup-Andersen, J. Mol. Spectroscopy **7**, 58 [1961].
[5] W. Gordy and R. L. Cook, Microwave Molecular Spectra, Interscience Publishers, New York 1970.
[6] S. Golden and E. Bright Wilson, Jr., J. Chem. Phys. **16**, 669 [1948].
[7] J. A. Pople and G. A. Segal, J. Chem. Phys. **43**, 136 [1965] and **44**, 3289 [1966].
[8] R. M. Lees, J. Mol. Spectroscopy **33**, 124 [1970].
[9] W. Kirchhoff, J. Mol. Spectroscopy **41**, 333 [1972].
[10] K.-M. Marstokk and H. Møllendal, J. Mol. Structure **8**, 234 [1971].
[11] D. R. Herschbach and V. W. Laurie, J. Chem. Phys. **37**, 1668 [1962].
[12] V. W. Laurie and D. R. Herschbach, J. Chem. Phys. **37**, 1687 [1962].
[13] D. R. Herschbach and V. W. Laurie, J. Chem. Phys. **40**, 3142 [1964].
[14] T. Oka and Y. Morino, J. Mol. Spectroscopy **8**, 9 [1962] and **11**, 349 [1963].
[15] R. K. Kakar, J. Chem. Phys. **56**, 1189 [1972].
[16] J. H. S. Green, Spectrochim. Acta **27 A**, 2015 [1970].

[17] M. Horak, I. J. Hyams, and E. R. Lippincott, Spectrochim. Acta **22**, 1355 [1966].
[18] J. E. Wollrab, Rotational Spectra and Molecular Structure, Academic Press, London 1967.
[19] J. H. Goldstein, J. Chem. Phys. **22**, 2078 [1954].
[20] H. Betsuyaku, J. Chem. Phys. **50**, 3117 [1969].
[21] F. A. Cotton and C. B. Harris, Proc. Nat. Acad. Sci. U.S. **56**, 12 [1966].
[22] J. M. Sichel and M. A. Whitehead, Theor. Chim. Acta (Berl.) **11**, 263 [1968].
[23] S. Eletr, Tae-kyu Ha, and C. T. O'Konski, J. Chem. Phys. **51**, 1430 [1969].
[24] D. W. Davies and W. C. Mackrodt, Chem. Comm. **1967**, 1226.
[25] M. J. S. Dewar, D. H. Lo, D. B. Patterson, and N. Trinajstic', Chem. Comm. **1971**, 238.
[26] P.-O. Löwdin, J. Chem. Phys. **18**, 365 [1950].

Frequencies and Temperature-Effects in the Vibrational Spectra of the Metal-Hydrate Complexes in $NiSnCl_6 \cdot 6\,aqu$ and in $NiSO_4 \cdot 6\,aqu$ *

J. Jäger ** and G. Schaack

Institut für Technische Physik der Technischen Hochschule Darmstadt

(Z. Naturforsch. **28 a**, 738–750 [1973]; received 15 January 1973)

We have investigated the internal vibrations of metal hydrate complexes in ionic single crystals and their interactions with the phonon system of the lattice, by observing the Raman spectra and infrared reflection spectra with polarized light at different temperatures T ($2\,K \leqq T \leqq 300\,K$). As special systems the octahedral nickel hydrate complexes in $NiSnCl_6 \cdot 6\,H_2O$, $NiSnCl_6 \cdot 6\,D_2O$ and in $NiSO_4 \cdot 6\,H_2O$, $NiSO_4 \cdot 6\,D_2O$ have been chosen. For $NiSnCl_6 \cdot 6\,aqu$ a complete interpretation of the spectra is given, starting from the assumption of isolated metal hydrate complexes and $SnCl_6^{--}$-ions as structural units. The discussion of the spectra of the sulfate crystal is based on the corresponding assumption. However, here an unambiguous assignment of all lines observed was not possible.

The most prominent feature of all spectra is the strong temperature dependence of the line widths which is much more pronounced than in anhydrous crystals in the same temperature interval. This effect is qualitatively explained in terms of the anharmonicity of the potential by which the water molecules are bound in the crystal lattice. Simple models for this potential are discussed.

Introduction

The problem of assigning infrared or Raman lines to certain lattice vibrations of the water molecules in hydrated ionic crystals in terms of translational and (or) librational modes has been discussed in several papers (e. g. [1, 2]). The central question is whether the hydrate complexes consisting of water molecules surrounding a central metal ion can be regarded as quasi-molecules in the sense of lattice dynamics, as they are regarded as structural units of the crystalline lattice. Additional interest in these problems arose since it was shown that the electronic excitation energy of rare earth and transition metal ions in hydrated crystals can be transferred to the lattice via the vibrational excitation of the shell of water molecules [3]. The relaxation times of the excited electronic states are thus determined in part by the density of the vibrational states of this surrounding shell. The efforts towards an observation and unambiguous assignment of all the transitions predicted by group theory for a hydrate complex of given symmetry have, however, not been completely successful even in cases where IR as well as Raman measurements were available, probably because these measurements had been performed at room temperature. Below about 800 cm^{-1} the room temperature spectra of hydrates are considerably broadened compared to the low temperature spectra. The effects are similar to those recently observed in the IR spectrum of beryll [4] at much higher temperatures and in the IR spectra of molten alkali nitrates and sodium nitrate [5]. Therefore a proper assignment of the observed lines to the expected lattice vibrations can be more easily achieved if the analysis is based on the low temperature spectra. Recently Lafont et al. have reported more complete measurements on this subject [2]. Spectra recorded in the intermediate tempera-

Reprint requests to Prof. Dr. G. Schaack, Institut für Techn. Physik der Techn. Hochschule Darmstadt, *D-6100 Darmstadt*, Hochschulstraße.

* A project of the Sonderforschungsbereich "Festkörperspektroskopie" Darmstadt-Frankfurt, financed by special funds of the Deutsche Forschungsgemeinschaft.

** Present address: Physikalisch-Technische Bundesanstalt, Braunschweig.